Available online at www.sciencedirect.com
ScienceDirect
Journal of Power Sources 175 (2008) 40–48
JOURNAL OF POWER SOURCES
www.elsevier.com/locate/jpowsour

An investigation into the effects of a nano-thick gold interlayer on polypyrrole coatings on 316L stainless steel for the bipolar plates of PEM fuel cells

Yan Wang, Derek O. Northwood *

Department of Mechanical, Automotive, and Materials Engineering, University of Windsor, 401 Sunset Avenue, Windsor, Ontario, Canada N9B 3P4

Received 16 August 2007; received in revised form 21 September 2007; accepted 21 September 2007
Available online 2 October 2007

Abstract

Polypyrrole is one of the most important conductive polymers because it is easily oxidized, water soluble and commercially available. Also, polypyrrole coatings have potential applications in batteries, fuel cells, electrochemical sensors, anti-corrosion coatings and drug delivery systems. In this study, a very thin gold layer was first coated on SS316L, and then a polypyrrole coating was laid on top. The nucleation and growth mechanisms of polypyrrole on the gold-coated SS316L were studied by electrochemical nucleation and growth techniques. SEM was used to characterize the polypyrrole coating morphology. Potentiodynamic tests were performed to determine the corrosion parameters of the polypyrrole coatings. Potentiostatic tests of the coated SS316L were conducted in simulated anode and cathode environments of a PEM fuel cell. The simulated anode environment was at a potential of about −0.1 V versus SCE purged with H_2 and the simulated cathode environment was at a potential of about 0.6 V versus SCE purged with O_2. After coating with Au and polypyrrole, the polarization resistance of SS316L is increased about six times, and the corrosion current density is decreased about seven times, compared to the base SS316L. Also, our calculations show that the metal ion concentration in solution for the polypyrrole/Au/SS316L had met the target of 10 ppm after 5000 h fuel cell operation.

Keywords: Gold interlayer; Polypyrrole; PEM fuel cells

1. Introduction

With escalating oil prices and increasing environmental concerns, increasing attention is being paid to fuel cell technology [1,2]. Proton exchange membrane (PEM) fuel cells (PEMFCs) are considered as promising candidates for transportation applications because of their lower temperature operation and fast start-up [3]. However, there are a number of barriers, e.g. price, weight and volume, which have prevented PEM fuel cells from being more widely used.

Bipolar plates are very important components in PEM fuel cells. They are designed to accomplish many functions, including: distribute the fuel and oxidant in the stack; facilitate water management within the cell; separate the individual cells in the stack; carry current away from the cell and facilitate heat management [4]. Currently, bipolar plates are made of non-porous graphite because of its chemical and thermal stability. However, its high price and difficulties in machining the gas flow channels present problems for non-porous graphite bipolar plates. Also, non-porous graphite is very brittle, and is therefore readily broken, such that H_2 and O_2 could leak into the whole fuel cell system, which is potentially dangerous for fuel cell operation. The proposed substitute materials for non-porous graphite include metallic and composite materials.

Metals have good mechanical properties and chemical stability, electrical conductivity and thermal conductivity and can be recycled. Furthermore, they can be easily stamped to a desired shape to accommodate the flow channels in the fuel cell. However, in a PEMFC environment, metals are prone to corrosion and the resulting metal ions can readily migrate to, and poison, the membrane [5]. The dissolved metal ions can lower the ionic conductivity of the membrane and, thus, the performance of the PEMFC. Furthermore, any corrosion layer will lower the electrical conductivity of the bipolar plates, and increase the potential

* Corresponding author. Tel.: +1 519 253 3000x4785; fax: +1 519 973 7007.
E-mail address: dnorthwo@uwindsor.ca (D.O. Northwood).

0378-7753/$ – see front matter © 2007 Elsevier B.V. All rights reserved.
doi:10.1016/j.jpowsour.2007.09.089

loss because of a higher electrical resistance [5]. Hence, in order to be suitable materials of bipolar plates, metals should have both a very high corrosion resistance and high electrical conductivity.

Conductive polymers are a new type of material, which has a high redox potential, and properties of both metals and plastics. Electrochemical polymerization of conductive polymers has received wide attention because of its simplicity and the fact that it is a one-step process [6]. In our previous research work [5], we coated polypyrrole on SS316L and concluded that in a simulated fuel cell environment, the corrosion current density was decreased by about one order of magnitude, and the polarization resistance was increased by about one order of magnitude, by coating with polypyrrole. However, the resulting metal ion concentration in solution was still too high for the target of PEM fuel cells.

In this study, a nano-thick Au layer was coated on SS316L prior to coating with polypyrrole. The aim of this study is to investigate the effects of this nano-Au interlayer on both the nucleation and growth mechanisms for the polypyrrole and the electrochemical characteristics of the polypyrrole/Au/SS316L.

2. Experimental details

2.1. Base material

SS316L was chosen as the base material primarily because of its good corrosion resistance and relatively low price. The chemical analyses of the SS316L used in this study are given in Table 1. The SS316L sheet was cut into samples 1.5 cm × 1.5 cm (area = 2.25 cm^2). An electrical contact was made to one side by means of nickel print. Then the contact side and the edges of the metal sample were sealed with epoxy resin, leaving one side for coating and characterization [7].

2.2. Au and polypyrrole coating

Before coating with Au, the SS316L specimens were polished on 240 grit silicon carbide grinding papers, rinsed in ethanol and hot-air dried. A nano-thick layer Au was coated on SS316L surface using a Polaron SC502 Sputter Coater and a 15 s coating time. The Au coating was about 10 nm thick, and the surface had a somewhat golden color after Au-coating. In the nucleation and growth study of polypyrrole, the electrolyte was a 0.02 M sulphuric acid and 0.02 M pyrrole solution, and the coating method used was a potentiostatic method, which is the standard investigative method for nucleation and growth. In the electrochemical studies, the polypyrrole was coated onto the Au-coated SS316L surface using a galvanostatic method. The coating current was 0.0005 A. The electrolyte used for this polypyrrole coating was a 0.1 M sulphuric acid and 0.1 M pyrrole solution. The electrochemical instrumentation employed was a Solartron 1285 potentiostat. A standard three-electrode system was used, in which a platinum electrode was used as the counter electrode and a saturated calomel electrode (SCE) as the reference electrode. The coating temperature was ambient temperature.

Table 1
The chemical compositions of SS316L (wt%)

Metal	SS316L
C	0.021
Mn	1.82
P	0.029
S	0.01
Si	0.58
Cr	16.32
Ni	10.54
Mo	2.12
Cu	0.47
N	0.03
Fe	Balance

2.3. Characterization of surfaces

In order to observe any surface morphology changes, the samples were examined using optical microscopy (Buehler Optical Image Analyzer 2002 System). The detailed features of the surface microstructures were characterized at high magnifications using an environmental scanning electron microscope (ESEM) facility with EDX (FEI Quanta 200F with a solid state backscattered detector (BSD)).

2.4. Electrochemistry

Potentiodynamic and potentiostatic tests were utilized to analyze the corrosion characteristics of uncoated and coated metals. In the potentiodynamic tests, samples were stabilized at the open circuit potential (OCP), then the potential was swept from −0.1 V versus OCP to 1.2 V versus SCE at a scanning rate of 1 mV s^{-1}. In order to simulate the working conditions of a PEMFC, potentiostatic tests were conducted at the anode, the applied potential was −0.1 V versus SCE purged with H_2 and at the cathode, the applied potential was 0.6 V versus SCE purged with O_2. The potentiodynamic and potentiostatic tests were conducted at 70 °C. The electrolyte was a 0.5 M sulphuric acid solution.

2.5. ICP-MS tests

An ICP-MS (Thermo Instruments X-7 Inductively Coupled Plasma Mass-Spectrometer) technique was used to determine the metal ion concentration after 10 h potentiostatic testing in both the simulated anode and cathode environments. Inductively coupled plasma mass spectrometry (ICP-MS) analyses were conducted using a high-sensitivity (In and U sensitivities are >1.2 × 108 cps ppm^{-1}) ThermoFisher Scientific (Mississauga, On, Canada) X series II quadrupole instrument. An ICP-MS can be thought of as four main processes, including sample introduction and aerosol generation, ionization by an argon plasma source, mass discrimination, and the detection system. For sample introduction, the aqueous solution was introduced via a Conikal nebulizer combined with Cyclonic spray chamber in the continuous flow mode using a SC-2 autosampler from ESI. After the sample entered the nebulizer, the liquid was broken up into a

fine aerosol by the pneumatic action of Ar gas flow (~1 L min^{-1}) dispersing the liquid into tiny droplets. Then, the spray chamber only allowed the small droplets to enter the plasma for dissociation, atomization, and finally ionization of sample's element components. In ICP-MS, a plasma consisting of ions, electrons and neutral particles is formed from argon gas. Then the hot plasma is used to atomize and ionize the elements in a sample. The resulting ions that successfully pass through a series of apertures (cones) were first accelerated by a high voltage potential gradient and are then passed through a series of focusing lenses into the high-vacuum quadrupole mass analyzer. The isotopes of the elements were identified by their mass-to-charge ratio (*m*/*e*) and the intensity of a specific peak in the mass spectrum is proportional to the amount of that isotope (element) in the original sample. The ion detector used in the ICP-MS system is the electron multiplier. ICP-MS analyses data reduction was conducted using Excel worksheets-based programs/macros written in Visual Basic. Multielements calibration standards and internal standards have been used in the analyses.

3. Results and discussion

3.1. Nucleation and growth mechanism of polypyrrole on Au-coated SS316L

Fig. 1 presents the nucleation and growth curves of polypyrrole on an Au-coated SS316L surface at different applied potentials. At 0.6 V, the coating current density is very low for the whole process. Therefore, the coating rate is very low at 0.6 V and we could not see any coating on the metal surface. At 0.8 V, the coating current density is about 2×10^{-3} A cm^{-2} and only decreases very slightly for the complete coating process. Therefore, the polypyrrole growth rate remains approximately constant. At 1.0 and 1.2 V, the coating current gradually decreased to a very small value. The area under the current density–time curve and *x*-axis was the largest at 0.8 V. Therefore, there was more polypyrrole coated on the Au-coated SS316L surface at 0.8 V. This is reasonable considering the nucleation potential is around 0.8 V. We cannot compare the nucleation and growth curves with the theoretical 2D and 3D nucleation and growth curves derived by Harrison and Thirsk [8] because there is no peak current density in the nucleation and growth curves of polypyrrole/Au/SS316L. However, for the polypyrrole/Au/SS316L, there was a peak current density at 0.6, 0.8, 1.0

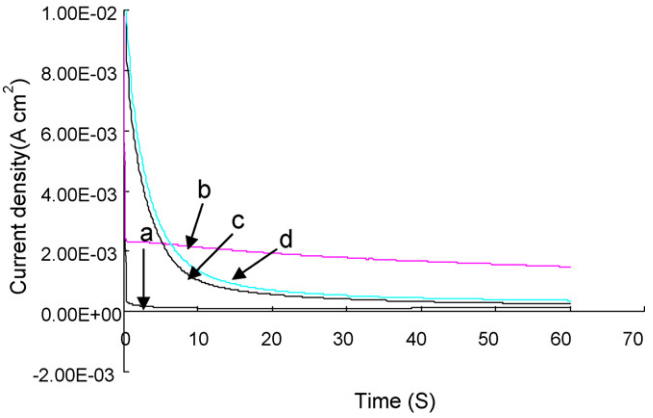

Fig. 1. Chronoamperometric curves of polypyrrole deposited on Au-coated SS316L at different potentials at ambient temperature: (a) 0.6 V, (b) 0.8 V, (c) 1.0 V, and (d) 1.2 V.

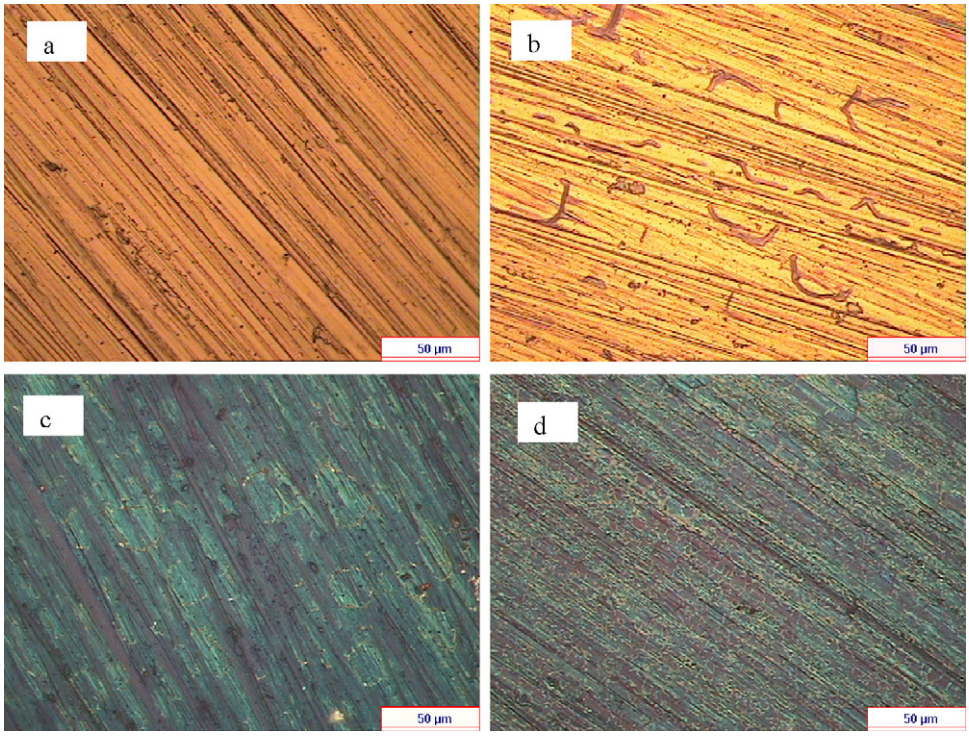

Fig. 2. Optical microscopy of polypyrrole coatings at different coating potentials for a 60 s coating time: (a) 0.6 V, (b) 0.8 V, (c) 1.0 V, and (d) 1.2 V.

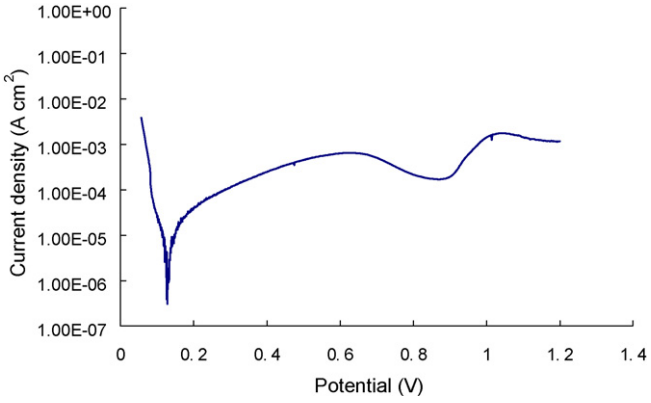

Fig. 3. Potentiodynamic curve for polypyrrole coating on Au-coated SS316L at 70 °C.

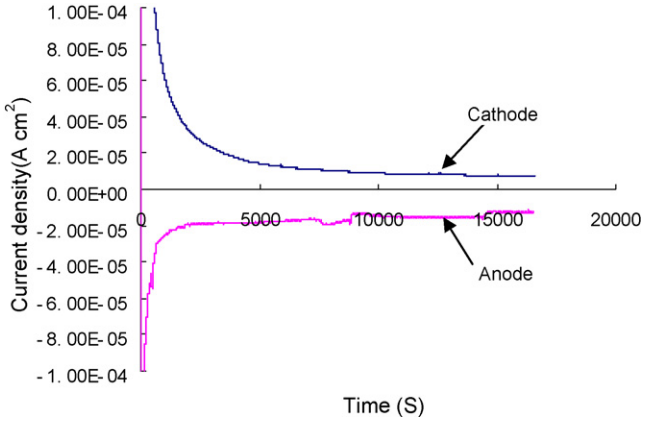

Fig. 4. Potentiostatic curve for polypyrrole coating on Au-coated SS316L in the simulated anode and cathode environments for PEM fuel cells.

and 1.2 V [9]. Taking the theoretical 2D and 3D nucleation and growth curves derived by Harrison and Thirsk [8] on the basis of current–time relationships, it was shown that before nuclei overlap, the nucleation and growth curves for polypyrrole on uncoated SS316L were in good agreement with a theoretical 3D instantaneous model and after nuclei overlap, the nucleation and growth curves remain more or less consistent with the theoretical curve for instantaneous 3D nucleation. In the nucleation and growth curves for polypyrrole on Au-coated SS316L, we cannot see the overlapping time because there is no peak current density in Fig. 1. Therefore, the base material affects the nucleation and growth of the polypyrrole coating. After coating with Au, the nucleation and growth characteristics of polypyrrole on Au-coated SS316L are different from those for uncoated SS316L.

3.2. Optical microscopy

Fig. 2 presents optical micrographs of the polypyrrole coatings produced on an Au-coated SS316L surface at different applied potentials. These micrographs were taken at the same brightness level so that the micrographs reflect any color differences (at 0.6 V because of the very small amount of polypyrrole, the brightness had to be reduced compared to 0.8, 1.0 and 1.2 V). In Fig. 2(a), we can only see the grinding marks on the surface. In Fig. 2(b), there are some "worm-like" polypyrrole particles beside the grinding marks. In Fig. 2(c) and (d), we can see that the polypyrrole particles have a globular shape. Comparing Fig. 2(b)–(d), we can see that the color of Fig. 2(b) is totally different from that for Fig. 2(c) and (d). Therefore, at the different coating potentials, the coating morphology is different. The color and morphology of the polypyrrole coatings produced at 1.0 and 1.2 V are similar, which is consistent with the chronoamperometric curves.

3.3. Potentiodynamic tests

Potentiodynamic tests were done to investigate the corrosion resistance of the polypyrrole/Au/SS316L. Fig. 3 presents the potentiodynamic curve of polypyrrole/Au/SS316L. From the linear polarization results, and using Eq. (1), we determined that the polarization resistance and corrosion current density were 1850 Ω cm^2 and 5.46 μA cm^{-2}, respectively.

$$R_p = \frac{\beta_a \beta_c}{2.3 i_{corr}(\beta_a + \beta_c)} \quad (1)$$

where β_a, β_c, i_{corr}, and R_p are the Tafel slopes of the anodic and cathodic reactions, the corrosion current density and polarization resistance, respectively [10].

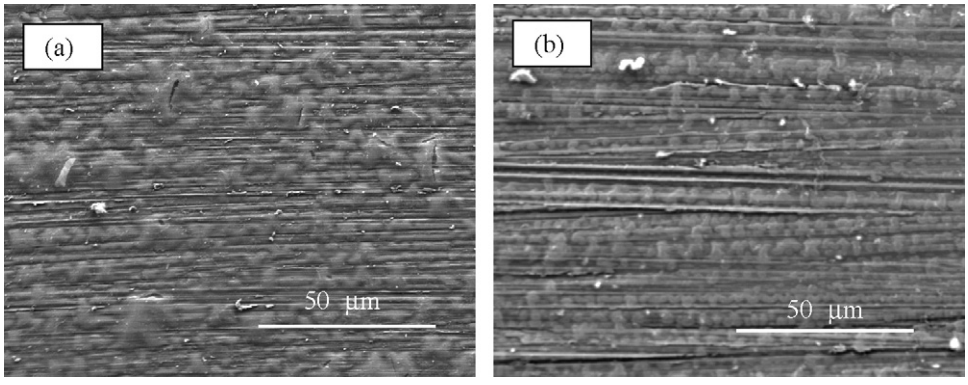

Fig. 5. SEM results after 10 h potentiostatic tests: (a) at −0.1 V vs. SCE purged with H_2 and (b) at 0.6 V vs. SCE purged with O_2 (secondary electron microscopy).

From our earlier research results for the same electrochemical test parameters [5,11], we had determined that the polarization resistance and corrosion current density of uncoated SS316L were 328 Ω cm^2 and 40 μA cm^{-2}, respectively. Therefore, after coating SS316L with Au and polypyrrole, the polarization resistance is increased about six times and the corrosion current density is decreased about seven times. Also, the corrosion potential of uncoated SS316L was about −0.25 V versus SCE,

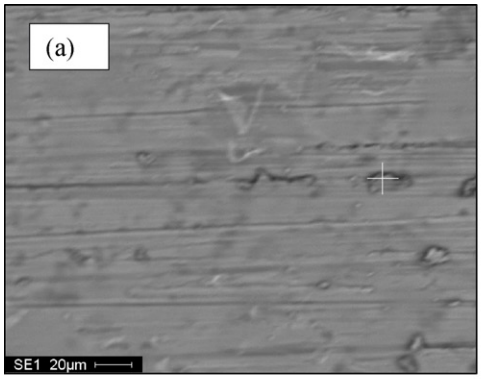

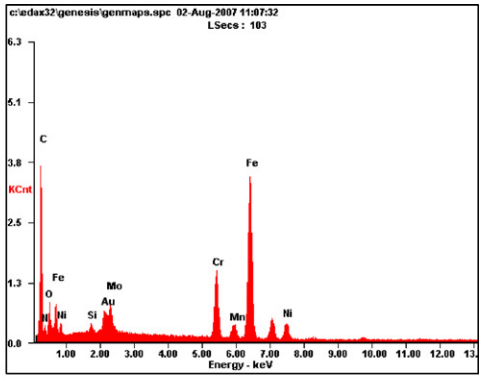

Element	Wt%	At%
CK	42.18	71.58
NK	03.68	05.36
OK	04.81	06.13
SiK	00.32	00.23
AuM	03.38	00.35
MoL	02.83	00.60
CrK	07.73	03.03
MnK	01.02	00.38
FeK	29.44	10.74
NiK	04.62	01.60
Matrix	Correction	ZAF

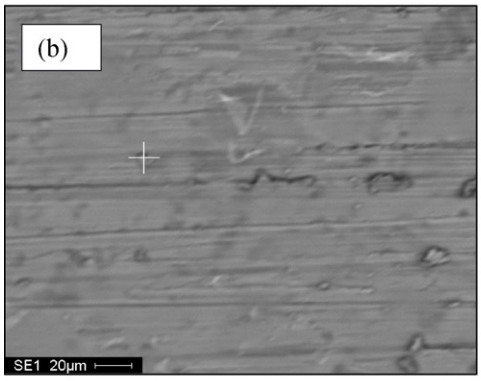

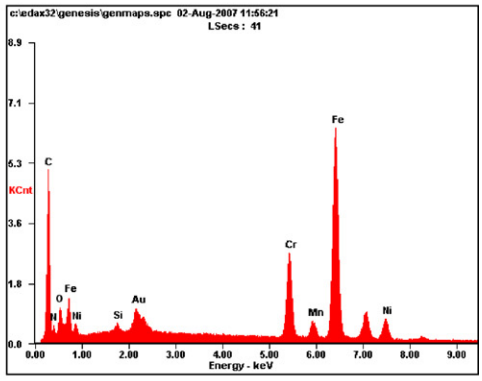

Element	Wt%	At%
CK	39.35	68.98
NK	04.35	06.53
OK	03.96	05.22
SiK	00.32	00.24
AuM	02.70	00.29
CrK	08.72	03.53
MnK	00.97	00.37
FeK	34.46	12.99
NiK	05.17	01.86
Matrix	Correction	ZAF

Fig. 6. SEM with EDX results after 10 h potentiostatic tests at −0.1 V vs. SCE purged with H_2, i.e anode (a) and (b) element analyses for one point, and (c) element analyses for the whole area (back-scattered microscopy).

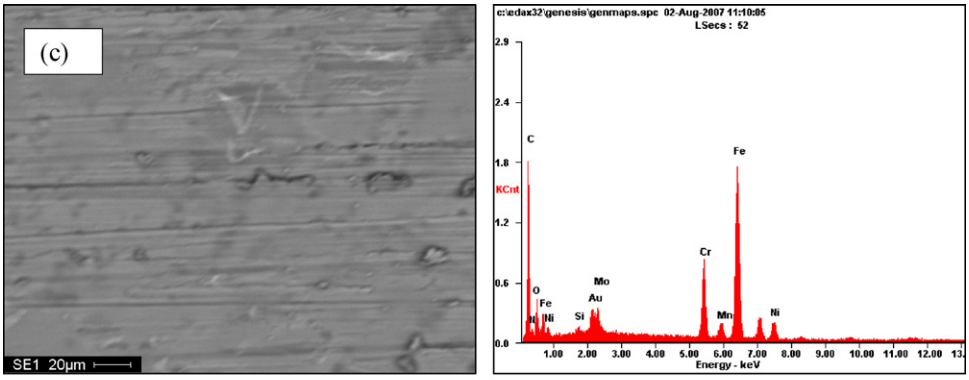

Element	Wt%	At%
CK	41.46	70.97
NK	03.46	05.08
OK	05.18	06.65
SiK	00.30	00.22
AuM	03.65	00.38
MoL	02.30	00.49
CrK	07.97	03.15
MnK	00.98	00.37
FeK	29.92	11.01
NiK	04.78	01.67
Matrix	Correction	ZAF

Fig. 6. (*Continued*).

whereas the corrosion potential of SS316L after Au and polypyrrole coating was about 0.1 V versus SCE. The corrosion potential is thus anodically shiftly, which therefore retards the corrosion of the base material. However, there was no passivation area after coating with Au and polypyrrole.

3.4. Potentiostatic tests

In the 'real' PEMFC working conditions, the anode is at a potential of about −0.1 V versus SCE and the cathode is at a potential of about 0.6 V versus SCE. Under these PEMFC conditions, any corrosion that takes place is not the same as free potential corrosion. In order to study the corrosion behavior of metallic bipolar plates in 'real' PEMFC working conditions, potentiostatic tests were conducted at −0.1 V versus SCE purged with H_2 to simulate the anode working condition and at 0.6 V versus SCE purged with O_2 to simulate the cathode working conditions. Although the setting time is 10 h for the potentiostatic tests, the software can only store 16,800 points (about 4.67 h) at 1 point s^{-1} speed. Therefore, Fig. 4 shows only a part of the total curve.

In the simulated anode conditions, the current density is quickly reduced to a negative value, then gradually increased to where the current density stabilized at about -2×10^{-5} A cm^{-2}. The stable current density is negative because H^+ changes to H_2. We have explained this behavior in detail in our previous papers [5,11–13]. This negative current density can provide either partial or complete protection for the metal at the anode. In the simulated cathode conditions, the current density was gradually reduced to a value of about 6–7 $\times 10^{-6}$ A cm^{-2}. Therefore, the corrosion is much more severe in the cathode environment than that in the anode environment.

Table 2
Metal ion concentration after potentiostatic tests for 10 h (the total solution volume is 100 ml)

Different coatings	Dissolved metal concentration (ppm)			
	Fe	Cr	Ni	Mn
Base solution	0.02	<IDL	<IDL	0.001
Uncoated SS316L at cathode side	1.25	0.23	0.18	0.04
Uncoated SS316L at anode side	0.77	0.13	0.08	0.02
Polypyrrole-coated SS316L at cathode side	0.66	0.06	0.09	0.02
Polypyrrole-coated SS316L at anode side	0.31	0.06	0.05	0.01
Polypyrrole- and Au-coated SS316L at cathode side	0.36	0.05	0.04	0.01
Polypyrrole- and Au-coated SS316L at anode side	0.32	0.05	0.02	0.01

IDL is identification limit.

3.5. SEM with EDX after 10 h potentiostatic tests

Fig. 5 presents secondary electron images of the polypyrrole coatings on Au-coated SS316L after the 10 h potentiostatic tests. We can readily see the particle shape of the polypyrrole, which is the same as that of polypyrrole/Au/SS316L (no Au) [5]. After 10 h potentiostatic testing in the simulated anode and cathode environments, the polypyrrole coating still completely covered the metal surface. Comparing Fig. 5(a) and (b), we cannot see any significant differences after 10 h

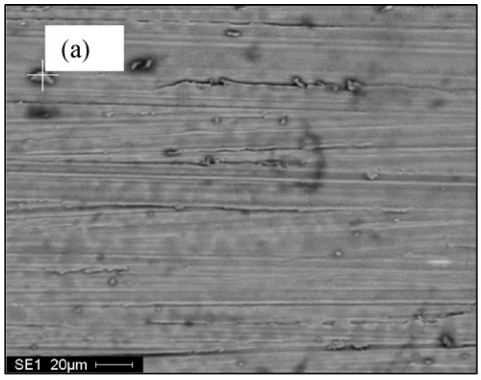

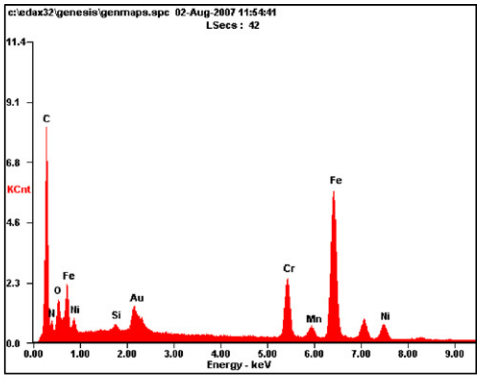

Element	Wt%	At%
CK	45.64	71.15
NK	06.48	08.67
OK	05.78	06.76
SiK	00.27	00.18
AuM	03.71	00.35
CrK	06.79	02.45
MnK	00.76	00.26
FeK	26.44	08.87
NiK	04.12	01.32
Matrix	Correction	ZAF

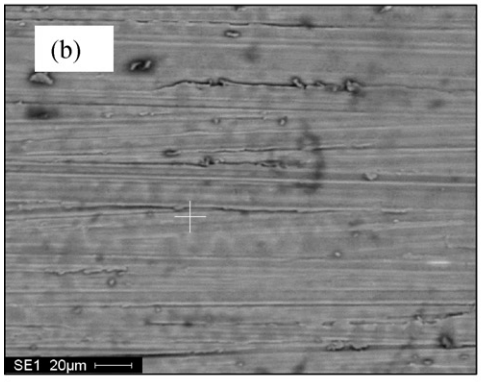

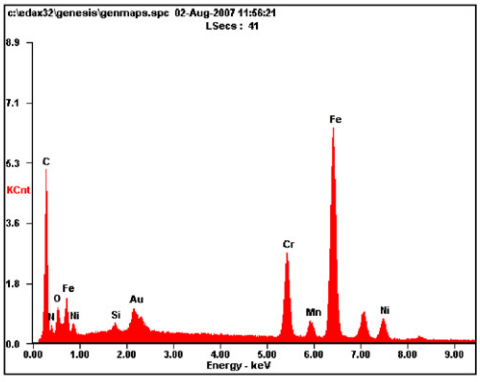

Element	Wt%	At%
CK	39.35	68.98
NK	04.35	06.53
OK	03.96	05.22
SiK	00.32	00.24
AuM	02.70	00.29
CrK	08.72	03.53
MnK	00.97	00.37
FeK	34.46	12.99
NiK	05.17	01.86
Matrix	Correction	ZAF

Fig. 7. SEM with EDX results after 10 h potentiostatic tests at 0.6 V vs. SCE purged with O_2, i.e cathode, (a) and (b) element analyses for one point, and (c) element analyses for the whole area (back-scattered microscopy).

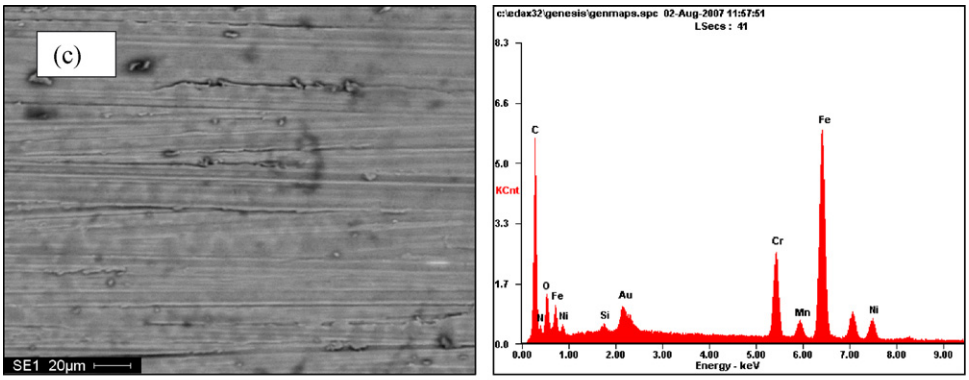

Element	Wt%	At%
CK	40.93	69.89
NK	03.89	05.70
OK	05.29	06.78
SiK	00.26	00.19
AuM	03.52	00.37
CrK	08.29	03.27
MnK	01.04	00.39
FeK	31.98	11.74
NiK	04.80	01.68
Matrix	Correction	ZAF

Fig. 7. (*Continued*).

potentiostatic testing in either the simulated anode or cathode environments. However, we have established (Fig. 4) that corrosion is more severe in the simulated cathode environment: these differences are not readily apparent in the SEM micrographs.

Fig. 6 presents the back-scattered electron images and EDX results for polypyrrole coatings in the simulated anode side. Fig. 6(a) and (b) are the elemental analyses for one point and Fig. 6(c) is the elemental analyses for the total area. From the elemental analyses, we can see the polypyrrole coating (C, N), the Au coating (Au) and the SS316L (Fe, Ni, Cr, Mn, Mo, Si). There are two possible sources of the oxygen (O) peak, one is because of the oxidation of SS316L and the other is oxidation of the polypyrrole. Therefore, the electrons for the EDX analyses penetrate through the polypyrrole and Au coatings into SS316L. Comparing elemental analyses in Fig. 6, we can see that some very small differences from point to point. Fig. 7 presents the back-scattered electron images and EDX results for the polypyrrole coatings in the simulated cathode side. Comparison of Figs. 6 and 7, shows little, or no, differences in elemental analyses.

3.6. ICP-MS

In a 'real' PEM fuel cell, metal ions generated from corrosion can migrate to the membrane and levels as low as 5–10 ppm can degrade the membrane performance [14–16]. Therefore, metal ion concentration in the solution is a very important parameter for the evaluation of the performance of metallic bipolar plates. The metal ion concentration in solution was determined after the potentiostatic tests. Table 2 shows us the metal ion concentration values in solution for the simulated anode and cathode conditions. Comparing the data in Table 2, we find that the metal ion concentrations at the cathode are higher than those at the anode for all elements for both uncoated SS316L and polypyrrole-coated SS316L. However, for polypyrrole/Au/SS316L, the metal ion concentrations are similar at the cathode and anode. Also, the polypyrrole/Au/SS316L exhibits the lowest metal ion concentration in solution. The polypyrrole-coated SS316L has a lower metal ion concentration in solution than for the uncoated SS316L. Therefore, based on our results, metal corrosion is more severe at the cathode environment, which is consistent with the potentiostatic test results and polypyrrole/Au/SS316L gives rise to the lowest metal ion concentration in solution.

PEM fuel cells should have operating lifetimes over 5000 h for transportation applications [17]. If, indeed, metal ion concentrations over 10 ppm can adversely affect membrane performance, then metal ion concentration build-up must not exceed 1 ppm 500 h^{-1}. Suppose that 5% of metal ions stay in solution, and then after 5000 h the total metal concentration in solution would be 24.45 ppm at the anode and 41.80 ppm at the cathode for uncoated SS316L. The metal ion concentrations would be 10.3 ppm at the anode and 20.1 ppm at the cathode after 5000 h for polypyrrole-coated SS316L. The metal ion concentrations would be 10 ppm at the anode and 11.5 ppm at the cathode after 5000 h for polypyrrole/Au/SS316L. Therefore, the Au/polypyrrole-coated material has met the target of 10 ppm after 5000 h of fuel cell operation.

4. Conclusions

Polypyrrole was successfully coated on the Au-coated SS316L. The nucleation and growth behavior of the polypyrrole coating on Au-coated SS316L was different from that observed for a polypyrrole coating on bare SS316L. The nature of the base material can therefore affect the nucleation and growth behavior of the polypyrrole coating. After coating with Au and polypyrrole, the polarization resistance of SS316L is increased about six times, and the corrosion current density is decreased about seven times, compared to the base SS316L. Also, the corrosion is much more severe in the PEMFC cathode environment than in the anode environment. From the ICP-MS results, we determined that the polypyrrole/Au/SS316L led to the lowest metal ion concentration in solution compared to uncoated SS316L and polypyrrole-coated SS316L. Our calculations show that the metal ion concentration in solution for the polypyrrole/Au/SS316L had met the target of 10 ppm after 5000 h fuel cell operation.

Acknowledgments

The research was financially supported by the Natural Sciences and Engineering Research Council of Canada (NSERC) through a Discovery Grant awarded to Prof. D.O. Northwood. Yan Wang acknowledges financial support through an Ontario Graduate Scholarship in Science and Technology.

References

[1] D.A. Boysen, T. Uda, C.R.I. Chisholm, S.M. Haile, Science 303 (2004) 68–70.
[2] Z. Zhan, S.A. Barnett, Science 308 (2005) 844–847.
[3] D.P. Davies, P.L. Adcock, M. Turpin, S.J. Rowen, J. Appl. Electrochem. 30 (2000) 101–105.
[4] A. Hermann, T. Chaudhuri, P. Spagnol, Int. J. Hydrogen Energy 30 (2005) 1297–1302.
[5] Y. Wang, D.O. Northwood, J. Power Sources 163 (2006) 500–508.
[6] D. Kumar, R.C. Sharma, Eur. Polym. J. 34 (1998) 1053–1060.
[7] H. Wang, J.A. Turner, J. Power Sources 128 (2004) 193–200.
[8] J.A. Harrison, H.R. Thirsk, in: A.J. Bard (Ed.), Electroanalytical Chemistry, vol. 5, Marcel Dekker, New York, 1971, p. 67.
[9] Y. Wang, D.O. Northwood, An investigation into the nucleation and growth of an electropolymerized polypyrrole coating on a 316L stainless steel surface, Thin Solid Films, submitted for publication.
[10] D.A. Jones, Principles and Prevention of Corrosion, first ed., Macmillan, New York, 1992, pp. 147.
[11] Y. Wang, D.O. Northwood, J. Power Sources 165 (2007) 293–298.
[12] Y. Wang, D.O. Northwood, Int. J. Hydrogen Energy 32 (2007) 895–902.
[13] Y. Wang, D.O. Northwood, Electrochim. Acta 52 (2007) 6793–6798.
[14] L. Ma, S. Warthesen, D.A. Shores, J. New Mater. Electrochem. Syst. 3 (2000) 221–228.
[15] M.P. Brady, K. Weisbrod, I. Paulauskas, R.A. Buchanan, K.L. More, H. Wang, M. Wilson, F. Garzon, L.R. Walker, Scripta Mater. 50 (2004) 1017–1022.
[16] M.J. Kelly, B. Egger, G. Fafilek, J.O. Besenhard, H. Kronberger, G.E. Nauer, Solid State Ionics 176 (2005) 2111–2114.
[17] R.G. Rajendran, MRS Bull. 30 (2005) 587–590.